

Fabrication of Metal Coated Carbon Nanotubes by Electroless Deposition for Improved Wettability with Molten Aluminum

Susumu Arai^{a*}, Yosuke Suzuki^a, Junshi Nakagawa^a, Tohru Yamamoto^a, Morinobu Endo^b

^aDepartment of Chemistry and Material Engineering, Faculty of Engineering, Shinshu University,
Nagano 380-8553, Japan

^bDepartment of Electrical and Electronic Engineering, Faculty of Engineering, Shinshu
University, Nagano 380-8553, Japan

*Corresponding author:

E-mail address: araisun@shinshu-u.ac.jp (S. Arai)

Tel: +81-26-269-5413 Fax: +81-26-269-5432

Abstract

Ni-P alloy coated and Au/Ni-P alloy double-coated multiwalled carbon nanotubes (MWCNTs) were fabricated using electroless plating. Three types of electroless Ni-P alloy plating baths were prepared to coat the MWCNTs with Ni-P alloy films of varying phosphorus content. Electroless gold coating of the Ni-P alloy coated MWCNTs was also carried out using a non-cyanide bath. The microstructures of the coatings on the MWCNTs were examined by scanning electron microscopy and X-ray diffraction. The wettability of the metal-coated MWCNTs with molten aluminum was also evaluated. MWCNTs coated with Ni-P alloy films containing 9-25 at.% phosphorus content were fabricated by electroless deposition. Electroless gold deposition on the Ni-P alloy coated MWCNTs to form Au/Ni-P alloy double-coated MWCNTs was also possible. The wettability of the metal-coated MWCNTs with molten aluminum was significantly improved compared to that of non-coated MWCNTs. The coating metals of the MWCNTs dissolved into the molten aluminum, resulting in good wettability between the MWCNTs and molten aluminum and dispersion of the resulting bare MWCNTs in the aluminum matrix. The dissolved coating metals formed stable compounds with molten aluminum.

Keywords: Multiwalled carbon nanotube, Electroless deposition, Wettability, Ni-P alloy, Au/Ni-P double-coating, Aluminum

1. Introduction

Carbon nanotubes (CNTs) [1,2] exhibit excellent mechanical characteristics (including high tensile strength and a high elastic modulus) and have high thermal conductivity. Consequently, CNT composites such as metal-CNT composites are expected to have high strength and high thermal conductivity. However, CNTs have poor wettability with molten metals such as aluminum. Applying a metal coating to CNTs is one of the most effective methods of improving their wettability with molten metals. Metal coating or deposition can impart various beneficial properties to CNTs, such as a high mean density, magnetic properties, and catalytic properties. A high mean density of metal coated CNTs can prevent the CNTs from becoming too easily airborne. CNTs coated with ferromagnetic metals can be controllably moved by magnetic fields, which may lead to CNT composites with highly controlled micro-textures [3]. CNTs deposited with catalytic metal particles may provide superior catalysts, with applications such as improved fuel cell electrodes [4]. Electroless deposition is a very effective and practical method of uniformly coating small powdery materials with metals [5-8]. Several investigations of the metal coating of CNTs by electroless deposition have been reported [9-14]. We have also reported that it is possible to coat CNTs with pure nickel [15], Ni-P alloy [16,17], Ni-B alloy [18], and copper [19] by electroless deposition. These metal-coated CNTs prepared by electroless deposition should improve the wettability of CNTs by molten metals. However, there have been very few reports on the effectiveness of the metal coating of CNTs in improving their wettability with molten metals. An experimental evaluation of the wettability of metal-coated CNTs by molten metals was required.

In the present study, Ni-P alloy coated CNTs and Au/Ni-P alloy double-coated CNTs fabricated by electroless gold deposition on Ni-P alloy coated CNTs were prepared by electroless deposition, and their wettability with molten aluminum was evaluated.

2. Experimental

2.1 Preparation of metal-coated CNTs

The CNTs used in the present study were commercially available vapor-grown multiwalled carbon nanotubes (MWCNTs: Showa Denko Co. Ltd.), formed via catalyst-assisted chemical vapor deposition and heat treated at 2800°C in argon gas for 30 min. The MWCNTs were typically 150 nm in diameter and 10 µm in length. Before electroless Ni-P alloy deposition, pre-treatment of the MWCNTs was carried out using a common two-step method (sensitization and activation). Because the MWCNTs were hydrophobic, 0.05 g of MWCNTs were initially dispersed in a 2×10^{-5} M polyacrylic acid (mean molecular weight of 5000: PA-5000) aqueous solution (0.05 dm³) with stirrer agitation and ultrasonic irradiation. By this treatment, the PA-5000 dispersants adsorbed onto the MWCNTs, making them hydrophilic. After the dispersion process, the MWCNTs were filtrated and rinsed, then immersed in a 4.4×10^{-2} M SnCl₂·2H₂O + 0.12 M HCl solution (0.1 dm³) at 25°C with agitation (ultrasonic irradiation: 1 min, stirrer agitation: 5 min) to adsorb Sn²⁺ ions on the MWCNTs (sensitization). After the filtration and rinse, the MWCNTs were immersed in a 5.6×10^{-4} M PdCl₂ + 0.12 M HCl solution (0.1 dm³) at 25°C with agitation (ultrasonic irradiation: 1 min, stirrer agitation: 5 min) to form palladium catalytic nuclei on the MWCNTs (activation). The electroless Ni-P alloy composite plating bath compositions used are shown in Table 1. Three different baths were prepared in order to form

Ni-P alloy films with different phosphorus contents. Sodium hypophosphite and sodium citrate were used as a reducing agent and a complexing agent, respectively. In order to homogeneously disperse the metal-coated MWCNTs in the plating baths, a stearyl trimethyl ammonium chloride dispersant was added to the plating baths. The pH of the low-phosphorus and medium-phosphorus baths was adjusted to 9. The pH of the high-phosphorus bath was adjusted to 7. Electroless plating was carried out at 30°C for the low- and medium-phosphorus baths and at 80°C for the high-phosphorus bath with stirrer agitation. The volume of all electroless Ni-P alloy plating baths was 0.5 dm³. The resulting Ni-P alloy coated MWCNTs were filtrated and rinsed. To fabricate Au/Ni-P alloy double-coated MWCNTs, the Ni-P alloy coated MWCNTs were placed in a non-cyanide electroless gold plating bath, which was called a substrate (Ni)-catalyzed electroless gold deposition bath [20]. The bath composition used in this study is shown in Table 2. This bath contained a sulfite and a thiosulfate as complexing agents for gold ions, and the thiosulfate was considered to be the main complexing agent [20, 21]. The sulfite acted as a reducing agent for gold ions on the nickel (nickel alloy) substrate surface, but not on the gold surface [20,22]. The bath pH was adjusted to 9. The volume of the bath was 0.5 dm³. Electroless gold deposition was performed at 60°C with stirrer agitation. All chemicals used were reagent grade, and pure water from an electro dialysis water purifier (RFP343RA, Advantec MFS, Inc.) was used in all experiments.

2.2 Characterization of the metal-coated MWCNTs

The microstructures of the deposits were examined using field-emission scanning electron microscopy (FE-SEM, JEOL JSM-7000F) and by X-ray diffraction (XRD, Shimadzu Seisakusho XRD-6000). The phosphorus content of the Ni-P alloy coatings was measured using electron probe X-ray microanalysis (EPMA, Shimadzu Co. EPMA-1610). A specialized sample

preparation system (Cross-section polisher, JEOL SM-09010) was used to prepare cross-sectional samples for FE-SEM observation.

2.3 Wettability of the metal-coated MWCNTs with molten aluminum

In the present study, pure aluminum (JIS H4160 A1N30) was used. The metal-coated MWCNTs were placed between a pure aluminum pan and a lid of the type generally used for thermal analysis, and then the pad/lid containing the metal-coated MWCNTs was pressed by an exclusive presser (Shimadzu Co. Model MHP-1), to form a wettability test sample. The weight of the pan/lid was around 20 mg, and that of the metal-coated MWCNTs was around 2 mg. A wettability test was carried out by analyzing cross sections of the test samples after heat treatment. The test sample was placed in a carbon container, and the heat treatment was performed using an infrared heating furnace (ULVAC Technologies Mila-3000) in vacuum at 700°C for 7.5 min. Because the melting point of the aluminum is 660°C, the pressed aluminum pan/lid melted and came into contact with the metal-coated MWCNTs as molten aluminum during the heat treatment. After the heat treatment, cross sections of the test samples were analyzed by SEM and EPMA.

3. Results and discussion

Figure 1 shows SEM images of Ni-P alloy coated MWCNTs. The reaction time was 15 min. Figure 1a shows the MWCNTs before the Ni-P alloy coating was applied. Figures 1b, 1c, and 1d are SEM images of Ni-P alloy coated MWCNTs using bath 1, bath 2, and bath 3, respectively. EPMA quantitative analysis indicated that the three coatings had phosphorus contents of 9, 14, and 25 at.%, respectively. Therefore, three kinds of Ni-P alloy coatings containing different phosphorus contents were formed on the MWCNTs by the electroless deposition technique. The

thicknesses of the Ni-9 at.% P alloy, Ni-14 at.% P alloy, and Ni-25 at.% P alloy films were approximately 150-200 nm, 150 nm, and 50 nm, respectively. The thicknesses of these coatings were controllable by changing the reaction time. The low and moderate phosphorus content Ni-P alloy coatings (Ni-9 at.% P and Ni-14 at.% P) were relatively uniform, whereas the high phosphorus content coatings were comparatively non-uniform.

Figure 2 shows XRD patterns of the Ni-P alloy coated MWCNTs shown in Fig. 1. The bottom XRD pattern is that of the MWCNTs before Ni-P alloy coating (Fig. 2d). A strong peak assigned to the MWCNT (002) plane was observed at 26.4 degrees. A broad peak assigned to the face-centered-cubic nickel (111) plane was visible for each XRD pattern around 44 degrees in addition to the MWCNT peak (Fig. 2a-c). The sharpness of the peak assigned to the face-centered-cubic nickel (111) plane decreased with increasing phosphorus content of the Ni-P alloy coating. Therefore, three Ni-P coatings with different phosphorus contents and different crystallinities were fabricated on the MWCNTs.

The Ni-P alloy coated MWCNTs were then coated with gold by electroless deposition using a thiosulfate-sulfite bath. Although gold deposition was possible on all three types of Ni-P alloy coated MWCNTs, the uniformity of the coatings decreased with increasing phosphorus content of the Ni-P alloy films. Since the electroless gold plating bath used in this study was a substrate (Ni)-catalyzed bath, the catalytic properties of the Ni-P alloy film might worsen with increasing phosphorus content of the Ni-P alloy film, or in other words, with decreasing nickel content of the Ni-P alloy film. Therefore, the reduction of the nickel content might decrease the uniformity of the gold coatings. Furthermore, in general, the phase structure of electroless Ni-P alloy plating films changed with increasing phosphorus content from a crystalline structure of face-centered-cubic nickel containing a small amount of phosphorus in solid solution to an

amorphous structure. As shown in Fig. 2, the crystallinity of the electroless Ni-P alloy plating films on CNTs became lower; that is, the phase structure of the Ni-P alloy plating films became more amorphous-like, with increasing phosphorus content of the films. This phase structure change of the Ni-P alloy films could affect the uniformity of the gold coating. Therefore, in the present study, low-phosphorus-content Ni-P alloy (Ni-9 at.% P alloy) coated MWCNTs were used for the fabrication of Au/Ni-P alloy double-coated MWCNTs.

Figure 3 shows XRD patterns of the resulting Au/Ni-P alloy double-coated MWCNTs at various reaction times. Compared to the XRD pattern of the Ni-P alloy coated MWCNTs (Fig. 3a: reaction time was 0 min), sharp peaks assigned to face-centered-cubic gold were visible at 38.1, 44.5, 64.6, and 77.6 degrees in addition to the peaks assigned to the MWCNTs (26.4 degrees) and the face-centered-cubic nickel of the Ni-9 at.% P alloy (around 44 degrees) (Fig. 3b: reaction time was 10 min and Fig. 3c: reaction time was 20 min). Therefore, gold was successfully deposited on the Ni-P alloy coated MWCNTs. The intensity of the peaks assigned to gold increased with increasing reaction time (Figs. 3b and 3c), but saturated after 20 min. Kato et al. reported that electroless gold deposition on an Ni-B alloy film substrate advanced primarily by a substrate(Ni)-catalyzed electroless gold deposition mechanism, with a minor contribution from a galvanic displacement reaction in the thiosulfate-sulfite bath [20]. Sato et al. reported that electroless gold films could also be produced on electroless Ni-P alloy film substrates using a thiosulfate-sulfite bath [22]. In the present study, the electroless gold deposition on the Ni-P alloy coatings of the MWCNTs probably occurred via the same mechanism.

Figure 4 shows cross-sectional SEM images (composition mode) of gold coatings on Ni-P alloy coated MWCNTs at different reaction times. White, gray, and black regions in the SEM images represent areas of deposited gold, Ni-9 at.% P alloy coating, and MWCNTs, respectively.

At 10 minutes, the gold deposited as particles, and the Ni-P alloy coatings were not uniformly coated with gold (Fig. 4a). At 20 minutes, the Ni-P coating was uniformly coated with deposited gold, which was approximately 50 nm thick (Fig. 4b). There were no gaps between the gold coating and the Ni-P alloy coating, or between the Ni-P alloy coating and the MWCNT. Furthermore, no voids were visible in the cross section of the Au/Ni-P alloy coated MWCNT. Therefore, a defect-free Au/Ni-P alloy double-coating was formed on the MWCNTs. After 20 minutes, the thickness of the gold films did not continue to increase. This is consistent with the XRD results (Fig. 3). As described above, the sulfite acts as a reducing agent for gold ions on nickel in the thiosulfate-sulfate bath [18]. Therefore, once the Ni-P coatings were completely covered with deposited gold, the gold coatings did not continue to grow. These results are consistent with Sato's report describing electroless gold deposition behavior on Ni-P alloy substrates using a thiosulfate-sulfite bath [22].

Ni-9 at.% P alloy coated MWCNTs and Au/Ni-9at.% P alloy double-coated MWCNTs were tested for wettability with molten aluminum. Figure 5a shows a cross-sectional SEM image of a wettability test sample of non-coated MWCNTs after heat treatment. The MWCNTs were not wet by the aluminum matrix at all, and the MWCNT layer remained in the aluminum matrix. Figure 5b shows a cross-sectional SEM image (composition mode) of a wettability test sample of Ni-P alloy coated MWCNTs after heat treatment. The thickness of the coating was approximately 200 nm. The black areas indicate cross sections of the MWCNTs, and the gray matrix area is aluminum. The MWCNT layer observed in Fig. 5a disappeared, and the MWCNTs dispersed individually throughout the aluminum matrix. There were no gaps between the MWCNTs and the aluminum matrix. Therefore, the Ni-P alloy coated MWCNTs were well-wetted by the molten aluminum. White and dark gray areas were also seen in Fig. 5b and the compositions of these

areas were unknown. In order to clarify the microstructure of the wettability test samples after heat treatment, EPMA mapping analysis was performed.

Figure 6 shows EPMA elemental mapping of the cross sections of wettability test samples of Ni-P alloy coated MWCNTs after heat treatment. The gray matrix area in the SEM image (back-scattering image) was aluminum. The black areas correspond to carbon, indicating that the MWCNTs were homogeneously distributed in the matrix. The white areas correspond to nickel. The dark gray areas correspond to phosphorus and oxygen. Since the distributions of carbon, nickel, and phosphorus were different, the MWCNTs were not coated with Ni-P alloy films after heat treatment, but bare MWCNTs were distributed throughout the matrix. The phosphorus in the Ni-P alloy coatings was believed to form phosphoric oxides such as P_2O_5 after heat treatment. The nickel in the Ni-P alloy coatings probably formed an Al-Ni intermetallic compound according to the Al-Ni binary alloy phase diagram [23].

Figure 7 shows a schematic of the reaction between Ni-P alloy coated MWCNTs and molten aluminum. During the heat treatment, the Ni-P alloy coating (that consists of nickel and phosphorus) completely dissolved into the molten aluminum, resulting in a good wettability between the molten aluminum, resulting in a good wettability between the molten aluminum and the Ni-P alloy coated MWCNTs (Fig. 7a). Consequently, the MWCNTs dispersed individually into the molten aluminum matrix. During coagulation, the dissolved nickel and phosphorus formed a stable Al-Ni intermetallic compound and a phosphoric oxide in the aluminum matrix, respectively (Fig. 7b).

Figure 8 shows the EPMA mapping analysis of a cross section of a wettability test sample of Au/Ni-9 at.% P alloy double-coated MWCNTs. The thicknesses of the Ni-P alloy coating and the

gold coating were approximately 150 μm and 50 nm, respectively. The distributions of aluminum, carbon, nickel, phosphorus, and oxygen were similar to those of the Ni-P alloy coated MWCNTs shown in Fig. 6. Bare MWCNTs were distributed across the matrix. Gold was also distributed across the matrix. The gold and some parts of the nickel distributions were similar. Gold and nickel form all proportional solid solution alloys [23]. Gold also forms several stable intermetallic compounds with aluminum, depending on the alloy composition [23]. Although gold may form ternary alloys such as Al-Au-Ni alloys, the exact composition and microstructure of the gold compound was unclear, as we are unaware of any information on the Al-Au-Ni ternary alloy phase diagram. Regardless, the Au/Ni-P alloy double-coated MWCNTs were well-wetted with molten aluminum.

Figure 9 shows a schematic of the reaction between the Au/Ni-P alloy double-coated MWCNTs and molten aluminum. During heat treatment, the gold coating first dissolved into the molten aluminum (Fig. 9a), and then the Ni-P alloy films (consisting of nickel and phosphorus) also dissolved into the molten aluminum (Fig. 9b), resulting in a good wettability between the MWCNTs and the molten aluminum. Consequently, the MWCNTs dispersed into the molten aluminum matrix. During the coagulation process, the dissolved gold, nickel, and phosphorus formed stable compounds such as Al-Au intermetallic compound, Au-Ni solid solution, Al-Ni intermetallic compound, and phosphoric oxide (Fig. 9c). In this study, since the wettability test was conducted in vacuum, it can be concluded that the Ni-P alloy coated MWCNTs and the Au/Ni-P alloy double-coated MWCNTs both showed good wettability with molten aluminum. However, the Au/Ni-P alloy double-coated MWCNTs should show superior wettability to the Ni-P alloy coated MWCNTs in atmosphere, due to the prevention of oxidation. In the future, we will evaluate the wettability of metal-coated MWCNTs with molten aluminum in atmosphere.

The metal coating of MWCNTs by electroless deposition is an effective technique to realize good wettability between MWCNTs and not only molten aluminum, but also other metals such as magnesium.

4. Conclusions

Ni-P alloy coated MWCNTs with various phosphorus contents were fabricated by electroless deposition. Gold coating of the Ni-P alloy coated MWCNTs was accomplished by electroless deposition using a non-cyanide bath. The Ni-P alloy coating and the Au/Ni-P alloy double-coating of MWCNTs significantly improved the wettability of MWCNTs with molten aluminum. This technique will be useful not only for molten aluminum, but also for other molten metals such as magnesium.

In the future, the effects of the dissolved nickel, phosphorus, and gold on the mechanical properties of the composites will be evaluated. Furthermore, the wettability of the metal-coated MWCNTs with molten metals will be evaluated in an air atmosphere.

Acknowledgements

This research was supported by Regional Innovation Cluster Program of Nagano, granted by MEXT, Japan.

References

- [1] A. Oberlin, M. Endo, and T. Koyama, *J. Cryst. Growth* 32 (1976) 335.
- [2] S. Iijima, *Nature* 354 (1991) 56.
- [3] D. Shi, P. He, P. Zhao, F. Fang Guo, F. Wang, C. Huth, X. Chaud, S. L. Bud'ko, and J. Lian, *Composites: Part B* 42 (2011) 1532.
- [4] Z. Liu, X. Lin, J. Y. Lee, W. Zhang, M. Han, and L. M. Gan, *Langmuir* 18 (2002) 4054.
- [5] W. S. Chung, S. Y. Chang, and S. J. Lin, *Plat. Surf. Finish.* 83 (1996) 68.
- [6] Y. J. Lin and B. F. Jiang, *J. Am. Ceram. Soc.* 81 (1998) 2481.
- [7] G. Wen, Z. X. Guo, and C. K. L. Davies, *Scripta Mater.* 43 (2000) 307.
- [8] C. Zhang, G. P. Ling, and J. H. He, *Mater. Lett.* 58 (2004) 200.
- [9] Q. Li, S. Fan, W. Han, C. Sun, and W. Liang, *J. J. Appl. Phys.* 36 (1997) L501.
- [10] J. Li, M. Moskovits, and T. L. Haslett, *Chem. Mater.* 10 (1998) 1963.
- [11] X. Chen, J. Xia, J. Peng, W. Li, and S. Xie, *Compos. Sci. Technol.* 60 (2000) 301.
- [12] M. Liebau, E. Unger, G. S. Duesberg, A. P. Graham, R. Seidel, F. Kreupl, and W. Hoenlein, *Appl. Phys. A* 77 (2003) 731.
- [13] W. X. Chen, J. P. Tu, L. Y. Wang, H. Y. Gan, D. Z. Xu, and X. B. Zhang, *Carbon* 41 (2003) 215.
- [14] Y. Zhao, Y. J. Xue, H. Zheng, and Y. X. Duan, *New Carbon Materials* 25 (2010) 65.
- [15] S. Arai, M. Kobayashi, T. Yamamoto, and M. Endo, *Electrochem. Solid-State Lett.* 13 (2010) D94.
- [16] S. Arai, M. Endo, S. Hashizume, and Y. Shimojima, *Electrochem. Commun.* 6 (2004) 1029.
- [17] F. Wang, S. Arai, and M. Endo, *Carbon* 43 (2005) 1716.
- [18] S. Arai, Y. Imoto, Y. Suzuki, and M. Endo, *Carbon* 49 (2011) 1484.
- [19] F. Wang, S. Arai, and M. Endo, *Electrochem. Commun.* 6 (2004) 1042.
- [20] M. Kato, J. Sato, H. Otani, T. Homma, Y. Okinaka, T. Osaka, and O. Yoshioka, *J. Electrochem. Soc.* 149 (2002) C164.
- [21] T. Osaka, M. Kato, J. Sato, K. Yoshizawa, T. Homma, Y. Okinaka, and O. Yoshioka, *J. Electrochem. Soc.* 148 (2001) C659.

- [22] J. Sato, M. Kato, H. Otani, T. Homma, Y. Okinaka, T. Osaka, and O. Yoshioka, J. Electrochem. Soc. 149 (2002) C168.
- [23] The Materials Information Society, Binary Alloy Phase Diagrams, 2nd ed., ASM International, Materials Park, OH (1996).

Figure Captions

- Fig. 1 SEM images of Ni-P alloy coated MWCNTs formed from various electroless deposition baths: (a) before electroless deposition, (b) low-phosphorus bath, (c) moderate-phosphorus bath, and (d) high-phosphorus bath.
- Fig. 2 XRD patterns of Ni-P alloy coated MWCNTs: (a) Ni-9 at.% P alloy coated MWCNTs, (b) Ni-14 at.% P alloy coated MWCNTs, (c) Ni-25 at.% P alloy coated MWCNTs, and (d) non-coated MWCNTs.
- Fig. 3 XRD patterns of Ni-P alloy coated MWCNTs after electroless gold deposition at various reaction times: (a) before electroless gold deposition, (b) 10 min, and (c) 20 min.
- Fig. 4 Cross-sectional SEM images of gold deposits on Ni-9 at.% P alloy coated MWCNTs at different reaction times: (a) 10 min and (b) 20 min.
- Fig. 5 Cross-sectional SEM images of wettability test samples after heat treatment using (a) non-coated MWCNTs and (b) Ni-9 at.% P alloy coated MWCNTs.
- Fig. 6 EPMA elemental mapping of the cross section of a wettability test sample of Ni-9 at.% P alloy coated MWCNTs after heat treatment.
- Fig. 7 A schematic of the wetting process between Ni-P alloy coated MWCNTs and molten aluminum: (a) dissolution of the Ni-P alloy coating (consisting of nickel and phosphorus) into molten aluminum during heat treatment, (b) formation of stable compounds such as Ni-Al intermetallic compound (Ni_xAl_y) and phosphorus oxide (P_xO_y) during coagulation.

Fig. 8 EPMA elemental mapping of the cross-sectional sample after wettability testing between Au/Ni-9 at.% P alloy double-coated MWCNTs and molten aluminum.

Fig. 9 Schematic of the wetting process between Au/Ni-P alloy double-coated MWCNTs and molten aluminum: (a) dissolution of gold coating into the molten aluminum during heat treatment, (b) dissolution of the Ni-P alloy coating (consisting of nickel and phosphorus) into the molten aluminum during heat treatment, and (c) the formation of stable compounds such as Au-Al intermetallic compound (Au_xAl_y), Au-Ni solid solution (Au-Ni), Ni-Al intermetallic compound (Ni_xAl_y), and phosphorus oxide (P_xO_y) during coagulation.

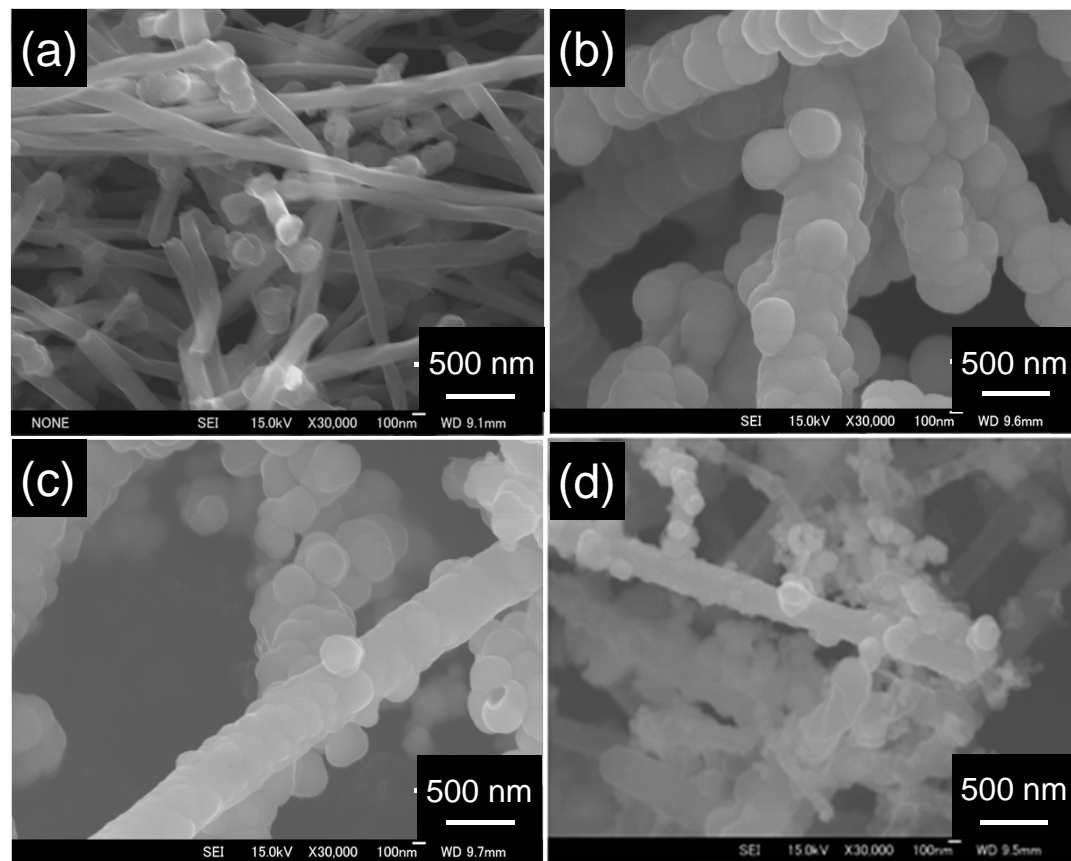


Fig. 1

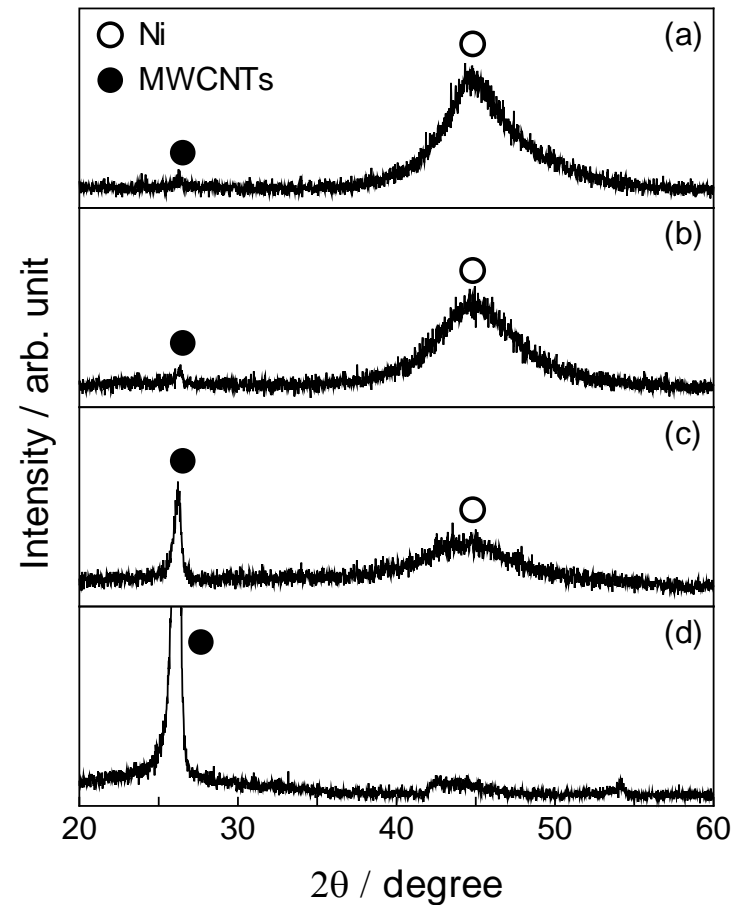


Fig. 2

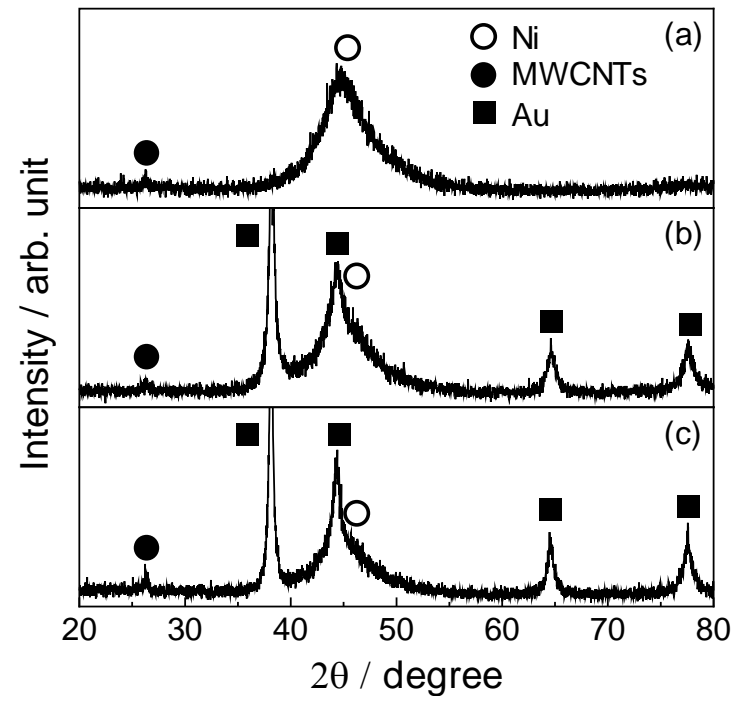


Fig. 3

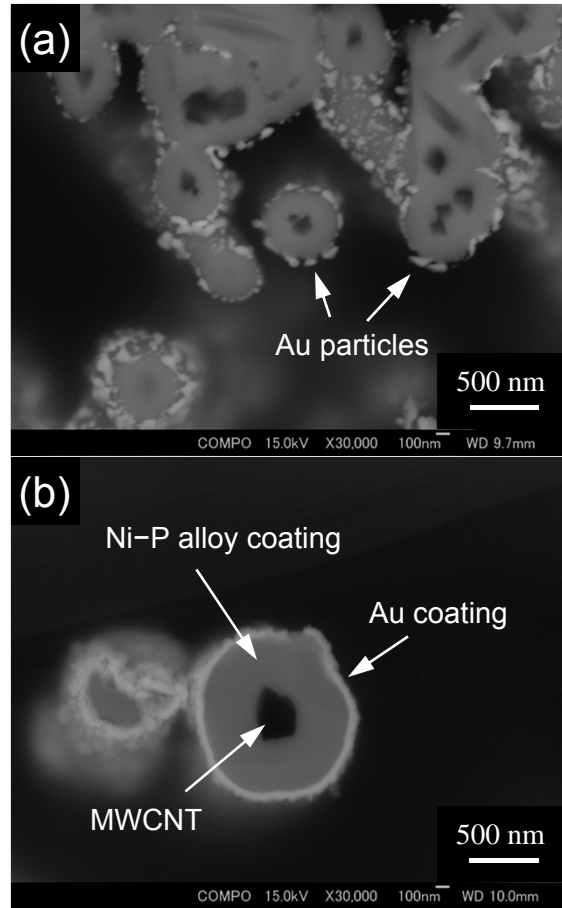


Fig. 4

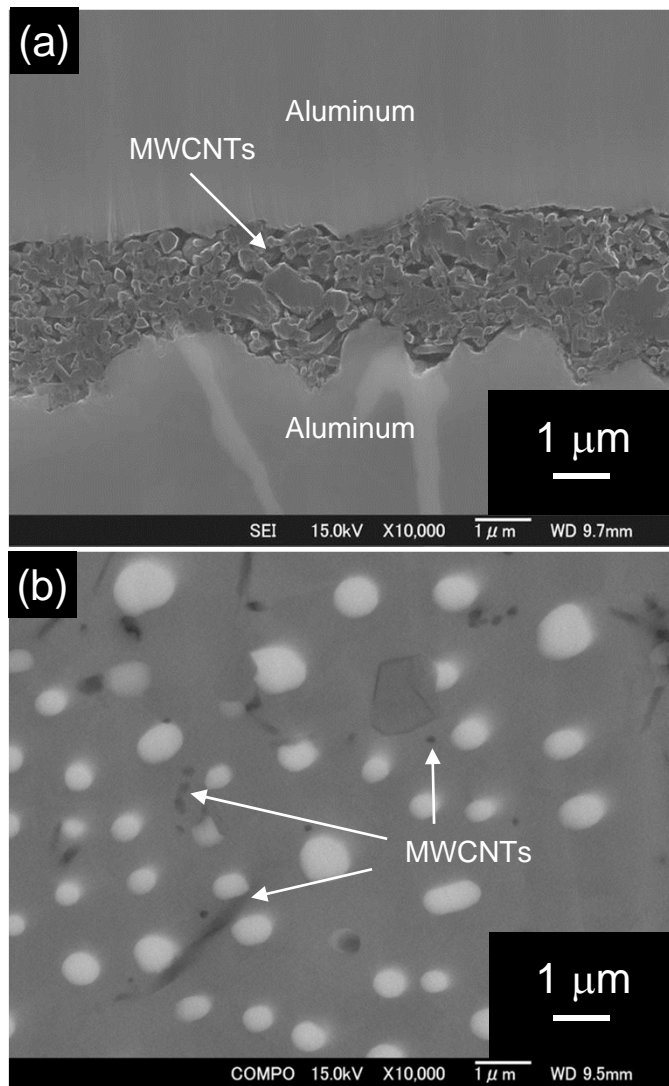


Fig. 5

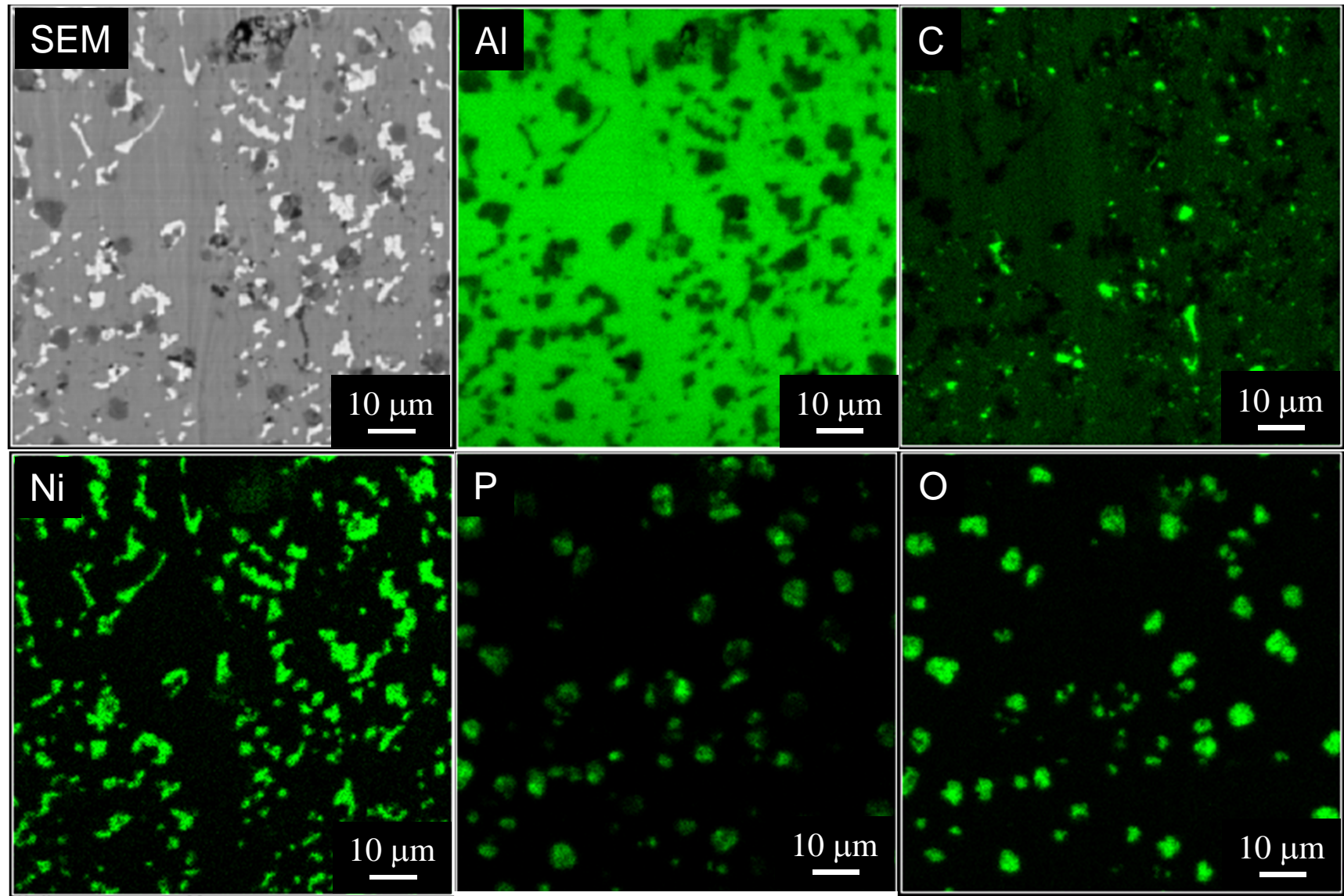


Fig. 6

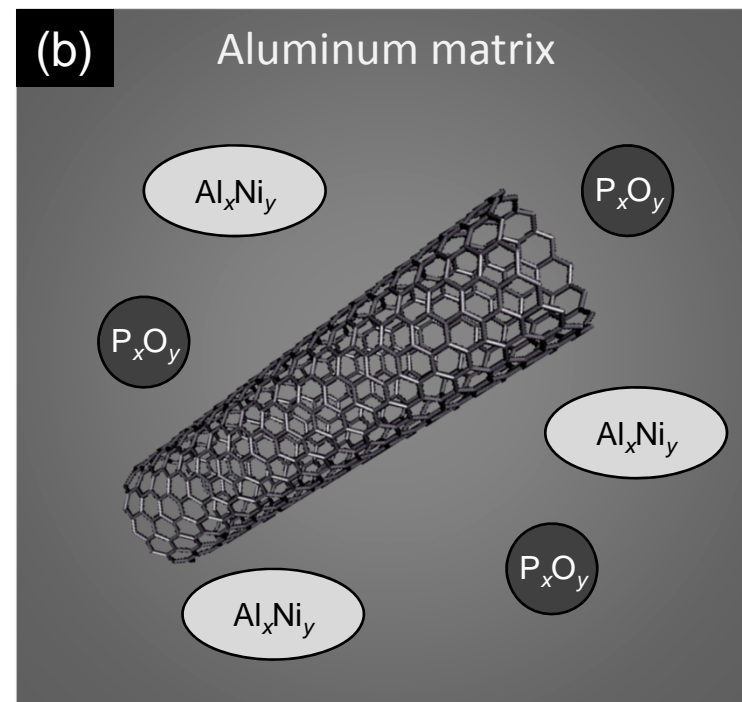
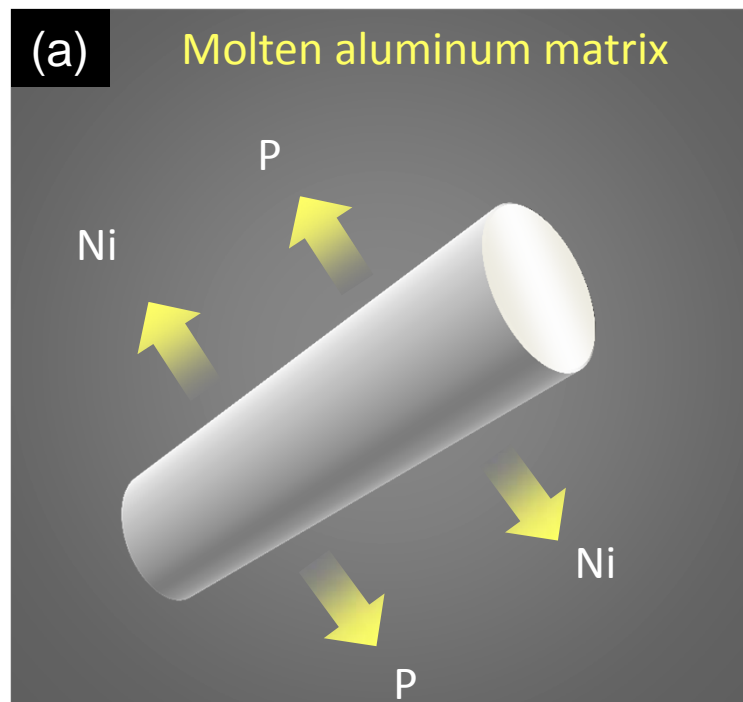


Fig. 7

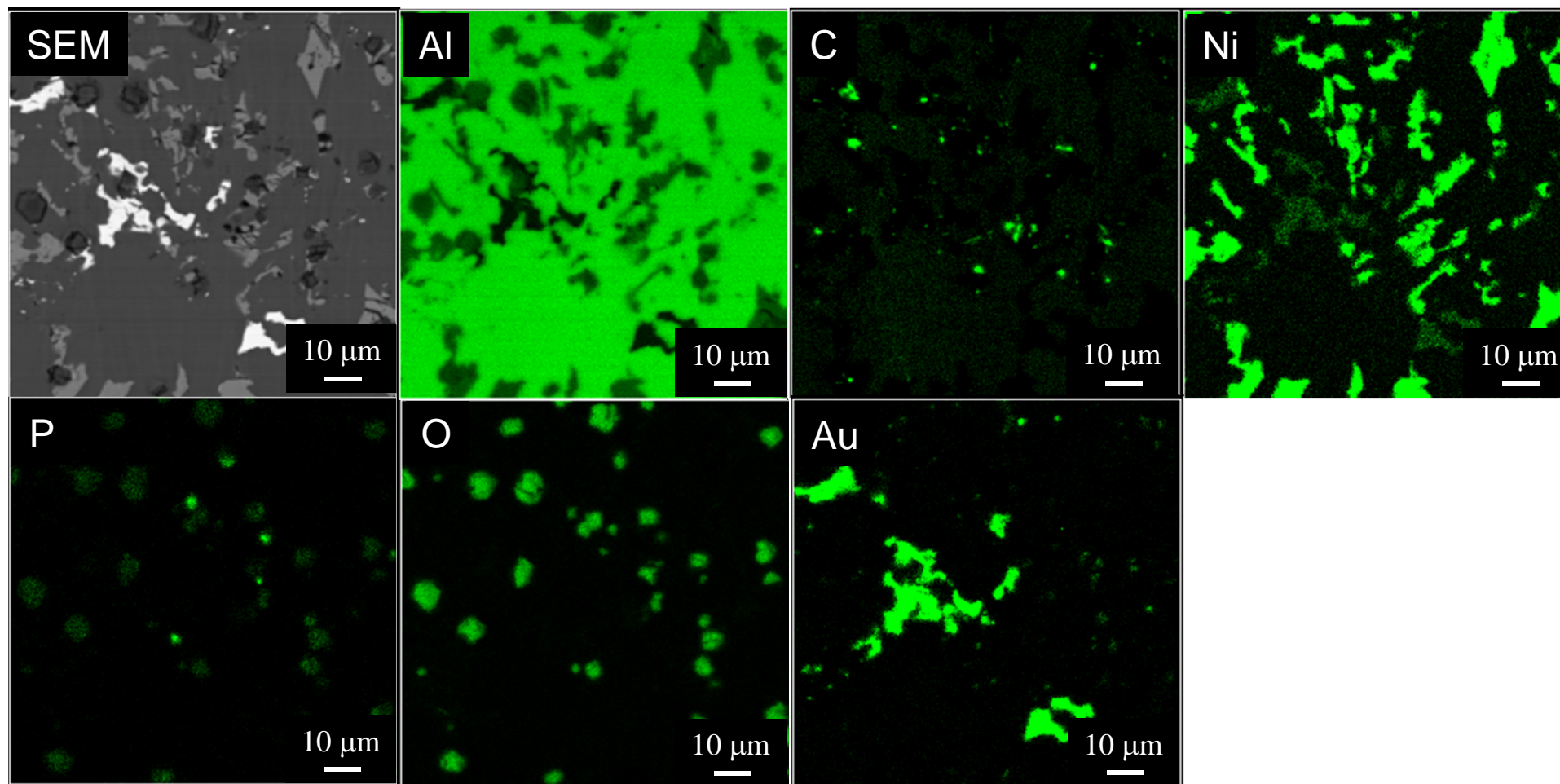


Fig. 8

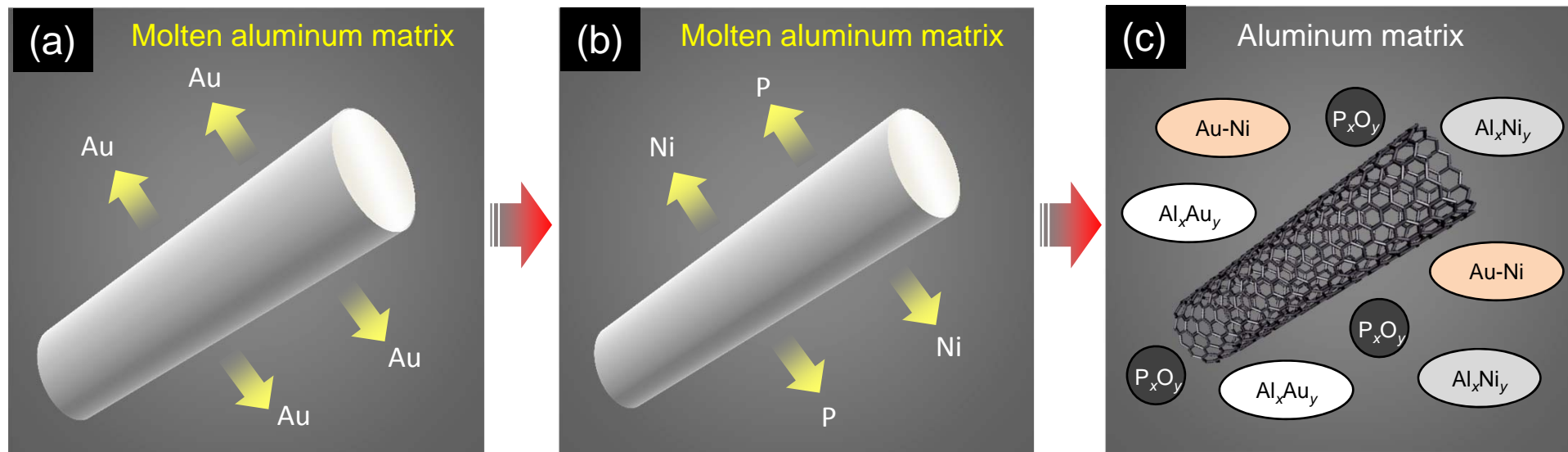


Fig. 9

Table 1 Bath compositions of electroless Ni-P alloy plating

Chemicals	Low-phosphorus	Moderate-phosphorus	High-phosphorus
NiSO ₄ ·6H ₂ O (M)	0.1	0.1	0.1
NaH ₂ PO ₂ ·H ₂ O (M)	0.2	0.2	0.2
C ₆ H ₅ Na ₃ O ₇ (M)	0.2	0.5	0.35
(NH ₄) ₂ SO ₄ (M)	0.5	0.5	0.5
Stearyl trimethyl ammonium chloride (M)	1×10 ⁻⁵	1×10 ⁻⁵	1×10 ⁻⁵

Table 2 Bath composition of electroless gold plating

Chemicals	Conc. (M)
NaAuCl ₄	0.01
Na ₂ SO ₃	0.32
Na ₂ S ₂ O ₃ ·5H ₂ O	0.01
Na ₂ HPO ₄	0.32